



## OPEN

# Rapid formation of multicellular spheroids in double-emulsion droplets with controllable microenvironment

SUBJECT AREAS:  
MESENCHYMAL STEM  
CELLS  
BIOMATERIALS - CELLS  
TISSUE ENGINEERING  
LAB-ON-A-CHIP

Hon Fai Chan<sup>1</sup>, Ying Zhang<sup>1</sup>, Yi-Ping Ho<sup>2</sup>, Ya-Ling Chiu<sup>1</sup>, Youngmee Jung<sup>1,3</sup> & Kam W. Leong<sup>1</sup>

<sup>1</sup>Department of Biomedical Engineering, Duke University, 101 Science Drive, Durham, NC 27708, USA, <sup>2</sup>Interdisciplinary Nanoscience Center (iNANO), Aarhus University, Aarhus C 8000, Denmark, <sup>3</sup>Center for biomaterials, Korea institute of science and technology, 14-gil 5 Hwarangno, Seoungbukgu, Seoul, 136-791, Korea.

Received  
7 October 2013

Accepted  
21 November 2013

Published  
10 December 2013

Correspondence and  
requests for materials  
should be addressed to  
K.W.L. (kam.leong@  
duke.edu)

An attractive option for tissue engineering is to use of multicellular spheroids as microtissues, particularly with stem cell spheroids. Conventional approaches of fabricating spheroids suffer from low throughput and polydispersity in size, and fail to supplement cues from extracellular matrix (ECM) for enhanced differentiation. In this study, we report the application of microfluidics-generated water-in-oil-in-water (w/o/w) double-emulsion (DE) droplets as pico-liter sized bioreactor for rapid cell assembly and well-controlled microenvironment for spheroid culture. Cells aggregated to form size-controllable (30–80  $\mu\text{m}$ ) spheroids in DE droplets within 150 min and could be retrieved via a droplet-releasing agent. Moreover, precursor hydrogel solution can be adopted as the inner phase to produce spheroid-encapsulated microgels after spheroid formation. As an example, the encapsulation of human mesenchymal stem cells (hMSC) spheroids in alginate and alginate-arginine-glycine-aspartic acid (-RGD) microgel was demonstrated, with enhanced osteogenic differentiation further exhibited in the latter case.

Multicellular spheroids recapitulate three-dimensional tissue *in vivo* in enabling cell–cell and cell–matrix interactions<sup>1</sup>. Cell–cell interactions regulate many biological processes such as development, homeostasis and disease progression via juxtacrine signaling mediated by direct cell contact or communication through functional junctions between cells<sup>2</sup>. Forming multicellular spheroids *in vitro* can establish cell–cell contact required for preserving cellular viability, function and phenotype that are often lost in monolayer culture<sup>3,4</sup>. In mesenchymal stem cell differentiation, aggregating cells to become spheroid or pellet is usually the prerequisite for efficient differentiation<sup>5</sup>.

The use of scaffold-free spheroids as microtissues for microscale tissue engineering presents many advantages and opportunities<sup>6–10</sup>, particularly with proliferative and pluripotent stem cell spheroids as building units for regenerative medicine. For instance, the differentiation of mesenchymal stem cells could be greatly enhanced with spheroid culture to facilitate tissue construction<sup>11</sup>. For microscale tissue engineering, the spheroid size and microenvironmental cues such as extracellular matrix (ECM) play an important role in directing stem cell behavior<sup>12,13</sup>. The size of mesenchymal stem cell (MSC) spheroid has been shown to influence its differentiation potential, with smaller spheroid directing more homogeneous chondrogenic differentiation towards hyaline chondrocytes whereas larger pellet producing more heterogeneous tissue<sup>14</sup>. Further, external microenvironmental cues in the form of matrix scaffold are often applied to direct stem cell differentiation. More precisely, the matrix scaffold can be modified to achieve desired mechanical properties or to present chemical and biological stimuli for controlled stem cell differentiation<sup>15–17</sup>. For examples, the encapsulation of MSC in poly(ethylene glycol) (PEG) hydrogel conjugated to RGD or hyaluronic acid hydrogel favors differentiation along the osteogenic or chondrogenic lineages, respectively<sup>18,19</sup>. The wide range of scaffold materials and modification options available suggests a need for a high-throughput system that can generate cell spheroids encapsulated in matrix scaffold efficiently.

Nevertheless, a scalable biofabrication technology for rapid, high-throughput production and yet offering a tunable microenvironment for spheroid culture is lacking. Conventional ways of making spheroids comprise culture in suspension, in spinner flask, or in hanging drop<sup>20</sup>. Culturing cells in suspension or in spinner flask is relatively simple but typically results in heterogeneity in spheroid size<sup>21</sup>. While culturing in hanging drop provides some control over the spheroid size, the technique is labor-intensive<sup>22,23</sup>. Although development such as high-throughput droplet printing could accelerate the spheroid production process, control issues of multiple aggre-



gates remain to be optimized<sup>24</sup>. Recently the research focus has turned to the approach of using non-adhesive micromolded surface<sup>25</sup>, taking advantage of microfabrication technique that supports spheroid size control as well as scaling up. However, the encapsulation of spheroid in matrix scaffold following its formation either requires multiple steps or replating<sup>12,26,27</sup>, complicating the process and possibly inducing spheroid fusion or damaging the mechanically weak spheroids due to shear stress induced by pipetting spheroids into ECM (e.g. hydrogel).

Microfluidics is to be a high-throughput yet miniaturized platform for performing biochemical and cell analysis<sup>28–33</sup>. Its high-throughput potential can be realized with the generation of microcompartmentalised water-in-oil (w/o) single emulsion droplets<sup>34,35</sup>. While the external oil phase of w/o emulsion is not compatible with cell culture applications as demonstrated by reduction in cell viability in single emulsion droplet culture<sup>36</sup>, the use of w/o/w double emulsion (DE) droplets circumvents the problem by introducing an outer aqueous phase to supply nutrients and oxygen for cell growth. One study reported the use of DE droplets as a programmable bioreactor to culture genetic modified *Escherichia coli* and analyze their inducible GFP expression by applying small molecule in the outer aqueous phase and allowing it to diffuse into the droplet core<sup>37</sup>. In this study

we demonstrate the use of w/o/w droplets for hMSC spheroid production via cell assembly and subsequent release as spheroid alone or encapsulation in microgel (Figure 1a). Although spheroid formation has been demonstrated with cells encapsulated in alginate or gelatin microgels generated by single-emulsion technology previously<sup>38–40</sup>, those techniques rely on some highly proliferative cell such as tumor cells to rapidly divide in the gel to form spheroids. We chose hMSC in this study since hMSC would not form a spheroid in an alginate gel normally<sup>41</sup>; serving the purpose to demonstrate the uniqueness of our spheroid formation technology. Importantly, the time required for spheroid formation of existing technologies is around 1 to 4 days<sup>23,38,40,42</sup>. In our approach, cells aggregate to form spheroid in 150 min. This rapid and versatile cell assembly technology should find many interesting stem cell tissue engineering applications such as in the field of cartilage and liver regeneration as well as high-throughput drug testing applications.

## Results

The high-throughput generation (>20 Hz) of pL-sized DE droplets was carried out in two polydimethylsiloxane (PDMS) flow-focusing devices connected serially (Supplementary Figure 1): the first device produced w/o emulsions (Figure 1b); the second device was used to

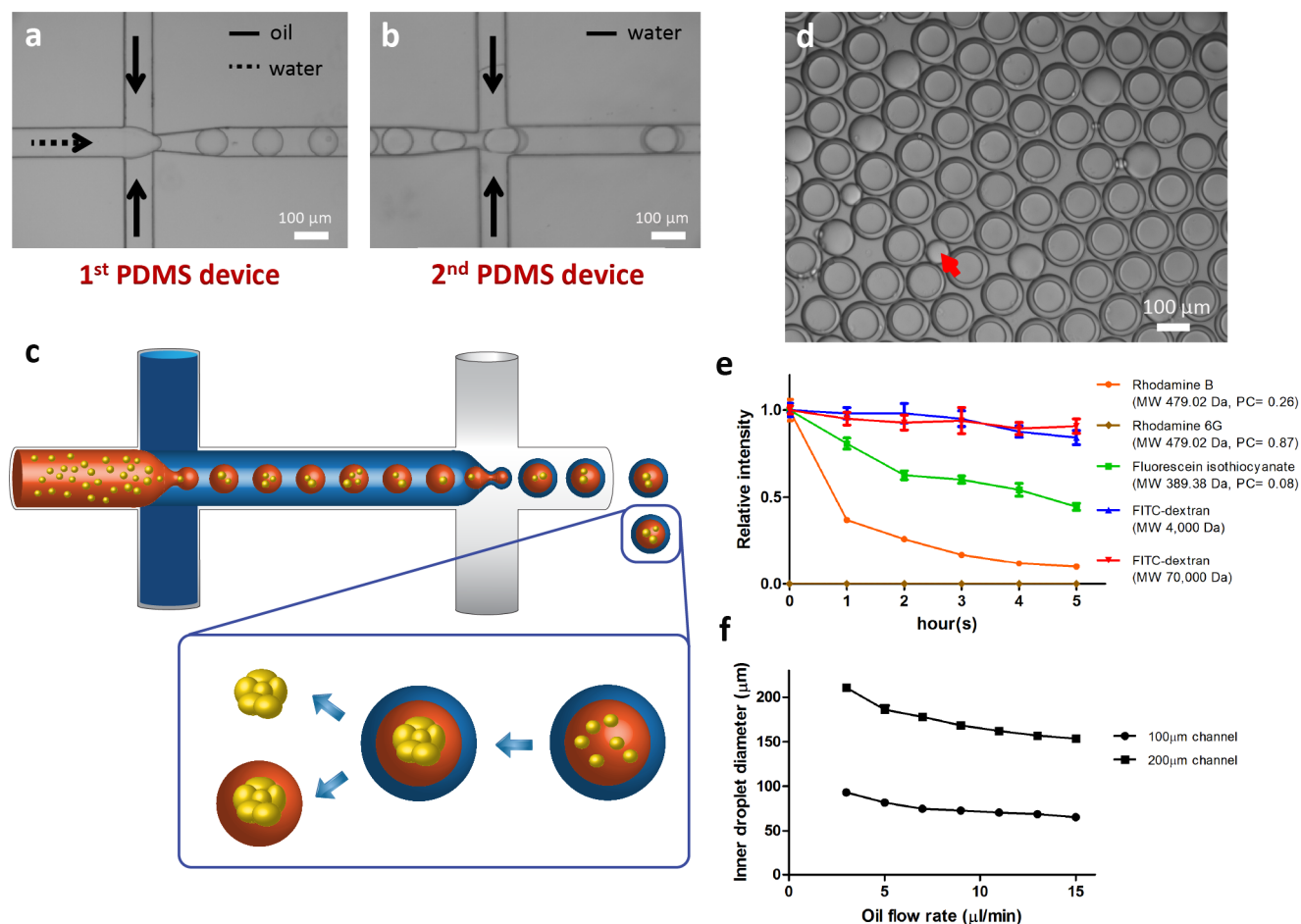


**Figure 1 | Generation and properties of DE droplets.** (a,b) Formation of w/o and w/o/w emulsions in two flow-focusing devices. (c) Schematic diagram showing how DE droplets are generated and spheroids are formed. Cells encapsulated in DE droplets assemble to form a single spheroid, which can be subsequently released with or without microgel encapsulation. (d) The appearance of DE droplets generated in device with 100  $\mu\text{m}$  channel width after collection. The red arrow indicates an empty oil droplet generated as side product. (e) Diffusion curve of different dyes encapsulated in DE droplets. Molecular weight (MW) and partition coefficient (PC) of the dyes are provided in the legend. (f) Size of core of DE droplets controlled by fixing inner aqueous phase flow rate at 2  $\mu\text{L}/\text{min}$  and altering oil phase flow rate ( $n \geq 30$ ). Figure 1C used with permission from Siying Ma.



supplement an outer aqueous phase to form w/o/w emulsions (Figure 1c and 1d). A small number of droplets with no inner droplet core or more than one droplet cores would be generated in the process. The probability of having one droplet co-encapsulated into one oil droplet is determined by a few factors, such as the relative flow rates of various phases, the dimension and configuration of the device and the presence of junk inside the channels. The occurrence of having no droplet co-encapsulated in an oil droplet (empty droplet) or more than one droplets co-encapsulated in an oil droplet seemed to exert little effect to the overall cell culture conditions (as cells were confined in the droplets they were situated in). We encapsulated various dyes or dextrans of different molecular weights conjugated with fluorescein isothiocyanate (FITC) inside the DE droplets and recorded the intensity of dyes in the core over time (Figure 1e and Supplementary Figure 2). A molecular weight-dependent diffusion of molecules out from the core was observed. Molecules with lower molecular weight (MW ~ 400 Da) were able to diffuse across the oil layer while larger molecules (MW ~ 70 kDa) were trapped within the droplets. Among molecules with similar molecular weight, their oil/water partition coefficient determines the permeability. Rhodamine 6G, rhodamine B and FITC with partition coefficient of 0.87, 0.26 and 0.08 diffused out from the droplets at a descending rate respectively. The selective permeability ensures nutrients to be delivered from the outer aqueous phase into the core and wastes to be removed in the opposite direction, thereby constituting an isolated bioreactor in each DE droplet for cell culture. The size of the “bioreactor”, or the droplet core, could be tuned by varying the flow rates of the inner aqueous phase versus the oil phase in the first device, or varying the microfluidics channel dimensions. As an example, two microfluidics devices with different channel widths (100  $\mu\text{m}$  and 200  $\mu\text{m}$ ) were used and the inner aqueous phase flow rate was fixed at 2  $\mu\text{L}/\text{min}$ . The diameter of the core of droplets could be tuned from 65  $\mu\text{m}$  to 90  $\mu\text{m}$  (100  $\mu\text{m}$  device) and from 150  $\mu\text{m}$  to 210  $\mu\text{m}$  (200  $\mu\text{m}$  device) by increasing the oil flow rate from 3  $\mu\text{L}/\text{min}$  to 15  $\mu\text{L}/\text{min}$  (Figure 1f). The polydispersity indexes of the droplet core were 0.027 and 0.022 for each case which suggested the droplet size was monodisperse. The tunability could be useful for controlling the number of cells inside the droplets and the size of microgel encapsulating the spheroids. Consistent with previously reported results, the distribution of number of cells in the droplets followed a Poisson distribution which provides a means to precisely control the number of cells in each droplet (Supplementary Figure 3a).

When hMSC were encapsulated and cultured in media, high cell viability was maintained for a period of four days (Supplementary Figure 3b). Culturing hMSC along with surfactant dissolved in the oil phase in 2D for one day led to aggregate formation, an effect that was not seen when cells were cultured with the oil alone (Figure 2a–c). In the DE droplets, cell assembly occurred rapidly within 150 min due to microscale confinement in the droplets that encouraged cell-cell interactions (Figure 2d). To demonstrate the versatility of this cell-clustering technology, we examined different cell types (PMEF, HepG2 and Caco-2). It took 2 hr for PMEF and HepG2 to form compact spheroid whereas Caco-2 required around 6 hr (Supplementary Figure 4a–d). The effect might be attributed to the differences in cell-cell affinity of various cell types. The frequency of spheroid formation in the droplets was nearly 100% (Supplementary Figure 5a). Compact spheroids (produced from any cell type) could be retrieved with the aid of a droplet-releasing agent (Figure 2e and 2f). The retrieval yield was above 95% (Supplementary Figure 5b) and high cell viability was maintained during the process.

The spheroid size could be controlled by changing the cell density used in the encapsulation process. In 200  $\mu\text{m}$  droplets, 2, 5, 10 and 20 million cells/mL density corresponding to 8, 20, 40, and 80 cells in each droplet on average, yielded spheroid size of 36, 46, 62, and 84  $\mu\text{m}$  on average, respectively (Figure 2g, Supplementary 5c and 5d). Larger spheroid size could be achieved by increasing the cell

density or the size of droplets so that more cells could be incorporated. Percentage of viable cell area within each spheroid ranged from 88% to 96% for various spheroid sizes (Figure 2h). The released spheroids displayed spherical shape, and attached and spread when cultured on low attachment surface and normal tissue culture plate, respectively (Figure 3a and 3b), consistently with findings from previous reports<sup>43</sup>. Furthermore, the released hMSC spheroids could be differentiated into adipogenic lineage more readily than cells cultured in 2D (Figure 3c and 3d), indicating the functionality of the cells was not affected after encapsulation. Apart from viability and differentiation capability, another measure of the “healthiness” of the spheroids is their endogenous ECM arrangement which modulates cell behavior such as adhesion, attachment and host response. To characterize hMSC spheroids generated from DE droplets, endogenous ECM molecules including collagen type I and laminin were stained in the spheroids to show that hMSC preserved and formed complex 3D network with their endogenous ECM in the spheroids, mimicking the situation *in vivo* (Figure 3e and 3f).

To demonstrate the feasibility of controlling the microenvironment for hMSC spheroid differentiation, hMSC spheroids were embedded in alginate or alginate-RGD microgel for osteogenic differentiation (Figure 4a). Specifically, hMSC suspended in alginate or alginate-RGD solution was adopted as the inner phase during the droplet formation process. Once spheroids were formed, they were released into a solution bath containing calcium ions. The contact between the alginate or alginate-RGD solution and calcium ions induced crosslinking among alginate molecules rapidly, leading to the formation of a solid gel. Phalloidin staining after 3-day culture of hMSC spheroids in the two different gels revealed similar cellular cytoskeletal organization and displayed no obvious changes in spheroid morphology (Figure 4b and 4f).

To determine the extent of cell-cell and cell-matrix interactions present in the spheroids in the microgels, immunostainings for E-cadherin, the transmembrane protein that regulates cell adhesion<sup>21,44</sup>, and integrin  $\alpha 5 \beta 1$  (the crucial attachment site for RGD sequence) were performed<sup>45</sup>. As shown in Figure 4c and 4g, both spheroids encapsulated in alginate or alginate-RGD gel displayed E-cadherin expression; however, hMSC spheroids encapsulated in alginate-RGD gel showed enhanced expression of integrin  $\alpha 5 \beta 1$  around the spheroids, suggesting the RGD sequence in the gel interacted with the spheroids actively to modulate its receptor expression, which could result in different cellular responses. One documented response is the enhanced osteogenic differentiation of MSC mediated by RGD sequence<sup>19</sup>. To show the applicability of our system in modulating stem cell differentiation, we induced osteogenic differentiation of hMSC spheroids encapsulated in alginate and alginate-RGD gels. After 7 days in culture, the spheroids in alginate-RGD gel contained more calcium deposits as shown by Alizarin red staining, and higher alkaline phosphatase activity, indicating enhanced osteogenic differentiation (Figure 4d, 4e, 4h and 4i)<sup>46</sup>. This example serves to validate our approach in controlling hMSC spheroid behavior by modulating its microenvironment.

## Discussion

The main difference between DE droplets and other microcapsule systems is that the microcapsule membrane which is often hydrogel itself is substituted with an oil layer<sup>47–49</sup>. In our case, no gelation step is involved when producing the droplets, which simplifies the encapsulation process and renders it unnecessary to control the viscosity of various phases to obtain a stable structure<sup>47,48</sup>. The choice of fluorinated oil (HFE-7500) as the oil phase with high oxygen permeability ensures adequate supply of oxygen<sup>50</sup>. The oil phase also serves as a selectively permeable barrier to encapsulate cells while allowing passage of small molecules across it, constituting a programmable bioreactor for cell culture<sup>37</sup>. On the other hand, the use of amphiphilic surfactant not only stabilizes the droplet structure but also induces

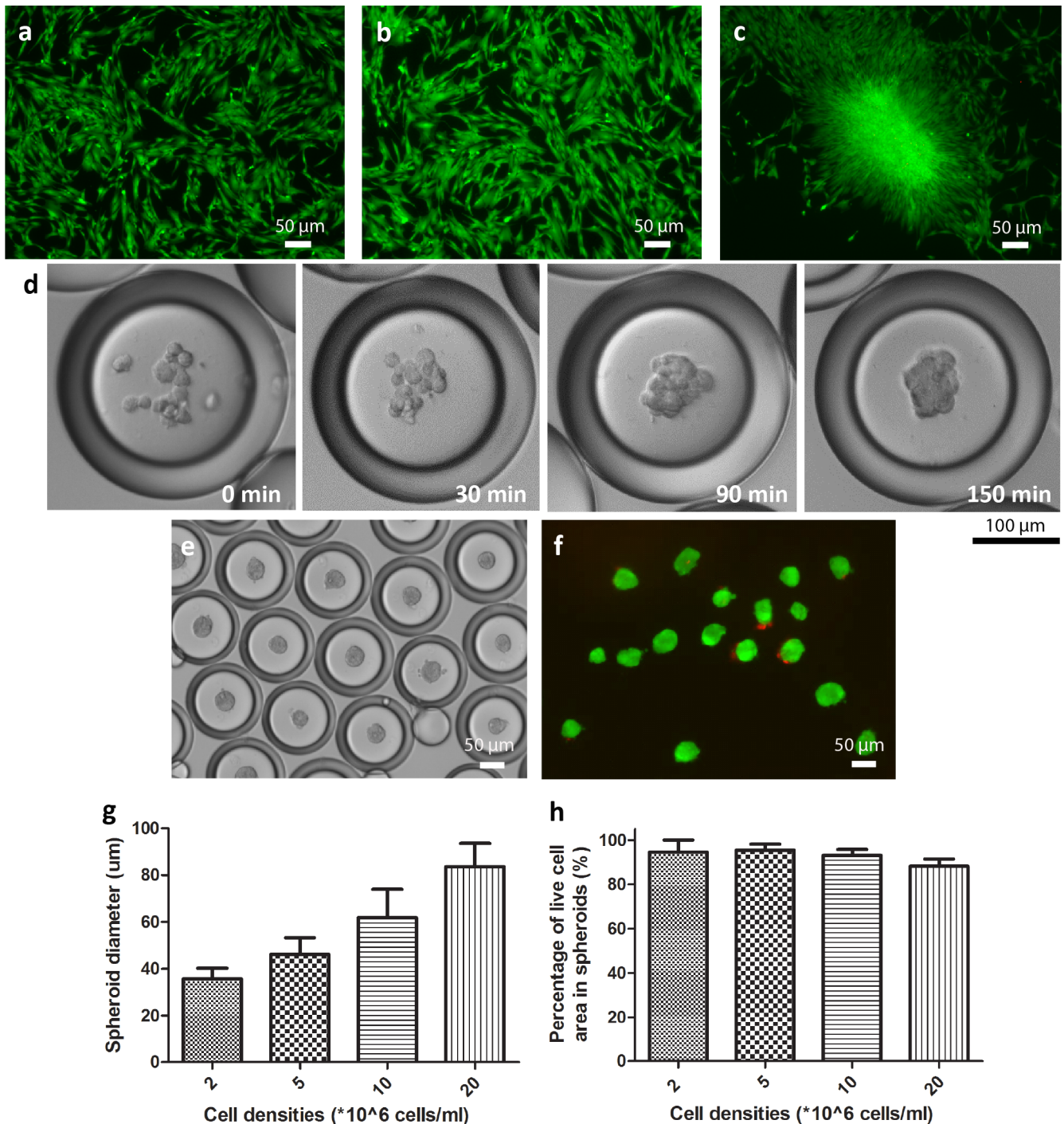


**Figure 2** | DE droplets generated in device with 200  $\mu\text{m}$  channel width as bioreactor for cell assembly. Live/dead staining of hMSC after monolayer culture for 1 day with (a) no addition of oil or surfactant, (b) with oil and (c) with 1% Pico-Surf<sup>TM</sup> 1 surfactant dissolved in oil. (d) Time course images showing spheroids are formed in 150 min. (e) Phase image of hMSC spheroids encapsulated in DE droplets after 6 hours. (f) Live/dead staining of spheroids after release from DE droplets at 6 hours. Live cells were labeled with calcein AM (green) and dead cells were labeled with propidium iodide (red). (g) Diameter of spheroids measured at different cell densities used ( $n \geq 50$ ). (Data = mean  $\pm$  SD) (h) Percentage of viable cell area in spheroids obtained at different cell encapsulation densities upon release ( $n \geq 10$ ). (Data = mean  $\pm$  SD).

rapid spheroid formation, i.e. 150 min in our case versus 1 to 4 days in existing technologies. We speculated that the surfactant (Pico-Surf<sup>TM</sup> 1) contains a hydrophilic end that performs similar function as polyethylene glycol to resist cell adhesion based on findings from previous reports<sup>51,52</sup>. Together with the microconfinement effect offered by the pico-liter sized droplets, these explain why cells aggregated rapidly to form spheroids in the DE. To support our claim, we synthesized PEG-PFPE surfactant following reported protocol and

generated DE droplets with it<sup>52</sup>. Similar effect of cell aggregation in the droplets was observed (Supplementary Figure 6). The spheroids generated by our approach, apart from using as microtissues for tissue regeneration<sup>53–55</sup>, offer other advantages such as better retention during implantation as well<sup>21,43</sup>. The technology may also prove useful in the drug testing application where rapid formation of microtissue such as hepatocyte spheroids allows high-throughput drug testing and screening.

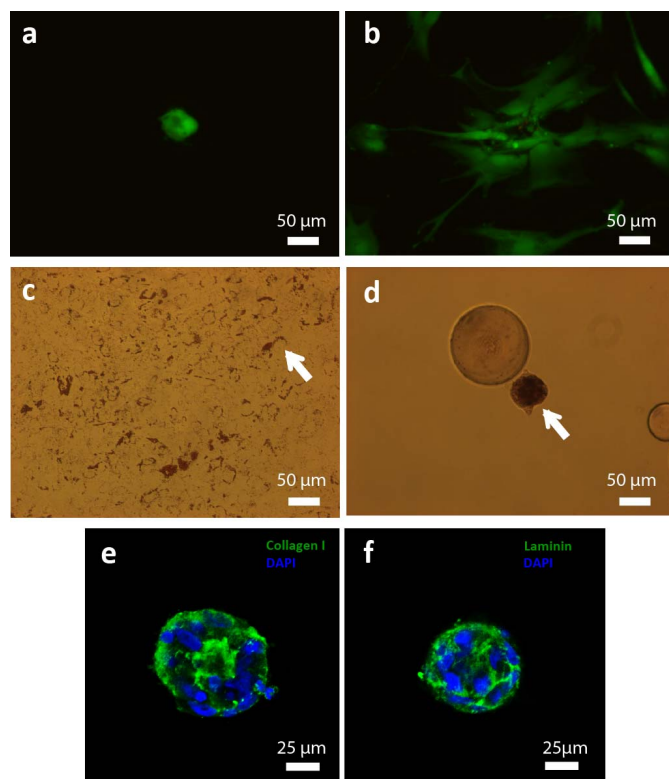


**Figure 3 | Characterisation of hMSC spheroids released from DE droplets.** Live-dead image of released hMSC spheroids cultured on (a) ultra-low attachment surface and (b) TCPS for one day (Green - calcein AM, red - propidium iodide). Oil Red O staining of hMSC cultured in (c) 2D and (d) 3D spheroid configuration differentiated along the adipogenic lineage for 7 days (Arrow indicates intracellular lipid vesicles). Immunofluorescence images of hMSC spheroid stained with (e) collagen type I and (f) laminin taken under confocal microscope.

The use of DE droplets as a cell analysis tool has previously been demonstrated by encapsulating genetic modified *Escherichia coli*<sup>37</sup>; however its potential in tissue engineering has not been studied. The more stringent requirement for mass transfer must be satisfied for mammalian cell culture. Therefore, we speculated that the gradual reduction in cell viability observed in DE droplets is due to large molecules such as growth factors that are prevented from entry across the oil layer. Nevertheless, as we have demonstrated, the formation of spheroid and its subsequent release or encapsulation inside a microgel could be accomplished within several hours, after which the oil layer can be removed to avoid the issue of mass transport impairment.

The general idea behind various approaches of inducing stem cell differentiation is to provide a biomimetic environment for directing stem cell differentiation into a particular lineage, often accomplished by the use of growth factors and exogenous matrix scaffold<sup>56</sup>. The DE droplets offer convenient control of the microenvironment where the inner aqueous phase can be easily tuned in microfluidics platform and is isolated from the outer aqueous phase. To accommodate the wide range of modulation options available, hydrogels such as collagen, agarose, gelatin and poly(ethylene glycol)-based hydrogels can be adopted as the inner phase<sup>57–59</sup>. Soluble ECM components such as laminin and fibronectin can also be incorporated to screen for the optimal ECM microenvironment and generate ECM-encapsulated spheroids at high frequency (>20 Hz in our case)<sup>60</sup>. The ease of entrapping spheroids in hydrogel directly in this study also circumvents the risk of dissociating or inducing fusion of spheroids during the transfer of spheroids into the hydrogel<sup>12</sup>.

Overall, this study demonstrates an innovative DE platform for rapid and high-throughput production of multicellular spheroids and modulation of their microenvironment. The platform can easily be scaled-up with multiple channels. The DE droplets, with their selectively permeable oil layer, serve as bioreactors for rapid cell assembly for hMSC and other cell types. The inner aqueous phase could be replaced with hydrogels to fine-tune the microenvironment for desired differentiation. The proposed platform obviates the need for labor-intensive fabrication of stem cell spheroids and replating of spheroids into matrix scaffold. This rapid, versatile and scalable cell assembly technology should help advance the field of microscale tissue engineering.

## Methods

**Microfluidics device fabrication.** Microfluidics devices were fabricated by conventional soft lithography techniques. The device design was drawn in AutoCAD and printed on transparencies to be used as photomask (CAD/Art Services, Inc., Bandon, OR). Patterned silicon mold of 200 µm in height was prepared from SU-8 2150 (MicroChem, Newton, MA) according to protocol. PDMS prepolymer and curing agent (Sylgard 184 Silicon Elastomer Kit, Dow Corning, Midland, MI) were mixed at 10 : 1 mass ratio before poured on top of the silicon mold. After curing at 75 °C for 1 hr, PDMS was peeled off from the mold before holes at inlets and outlets were punched (Hole puncher, Technical Innovations, Brazoria, TX). A cover slide was bonded with the device after oxygen plasma treatment for 40 s at 20 W (Plasma Asher, Quorum Technologies, West Sussex, RH). To create a hydrophilic surface along the channels, the devices were coated following a two-step sol-gel coating procedure<sup>37</sup>. (All chemicals listed below were obtained from Sigma-Aldrich, St. Louis, MO.) Briefly, the sol-gel solution was prepared from tetraethylorthosilicate (TEOS), methyltriethoxysilane (MTES), (heptadecafluoro-1,1,2,2-tetrahydrodecyl)-triethoxysilane, trifluoroethanol and 3-(trimethoxysilyl)-propylmethacrylate at a volume ratio of 2 : 1 : 4 : 1. Sol-gel solution, methanol, trifluoroethanol and hydrochloric acid solution (pH = 2) was mixed at a volume ratio of 5 : 9 : 9 : 1 and heated at 85 °C for 2 min. The activated mixture solution was filled to the devices after bonding with cover slide and the device was heated to 180 °C for 1 min. Finally, de-ionized water (500 mL), acrylic acid (200 mL), ammonium persulfate (10 wt%, 100 mL), and tetramethylethylenediamine (TEMED) (16 mL) were mixed and injected continuously to the devices at 20 mL/min while the device was heated at 80 °C for 10 min.

**DE droplets generation and characterization.** DE droplets were generated as described in the main text. Cell culture medium or alginate solution (1%) supplemented with Pluronic® F-127 (1 wt%) (Sigma-Aldrich, St. Louis, MO) was used as the inner aqueous phase. The oil phase used was HFE-7500 (Miller-Stephenson Chemical Co. Inc., Danbury, CT) supplemented with Pico-Surf™ 1 surfactant (1%) (Dolomite Microfluidics, Charlestown, MA). The outer aqueous phase comprised culture medium supplemented with Pluronic® F-127 (2.5 wt%). The flow rates of inner aqueous phase (3,5,7,9,11,13 µL/min), middle oil phase of HFE7500 (3 M, St. Paul, MN) (2 µL/min) and outer aqueous (6, 10, 14, 18, 22, 26 µL/min) were controlled by a Harvard Apparatus PHD 2000 Syringe Pump. To study the mass transport through the oil layer, various dyes (rhodamine B, rhodamine 6G, FITC) or dextran conjugated to FITC (MW = 4000 Da & 70000 Da) (50 µM) (all obtained from Sigma-Aldrich, St. Louis, MO) (50 µM) were prepared and encapsulated in the droplets. Images were taken at various time points using a Nikon Eclipse TE2000-U fluorescence inverted microscope fitted with appropriate filters and connected to a camera. The optimal exposure time for each dye was determined at time 0 and the same exposure time was used for the following time points. All other parameters (no binning, same lamp intensity, same brightness/contrast level) were kept the same during the course of experiments. The intensity of the core of at least 10 droplets was measured at different time points using ImageJ software (NIH). To determine the partition coefficient of various molecules, culture medium (with 20% FBS) containing rhodamine B, rhodamine 6G or FITC (50 µM) was added on top of HFE7500 containing Pico-Surf™ 1 (1%) in an eppendorf tube. The tube was left on an orbital shaker operating at 100 rpm for 24 hr before the fluorescent signal in the aqueous phase was determined by a plate reader. The amount of fluorescent dye left in the aqueous phase was determined by interpolation from a standard curve. Partition coefficient was calculated by the following formula: Partition coefficient = (Initial dye concentration – dye concentration after incubation)/Initial dye concentration.

**Culture and encapsulation of hMSC.** Bone marrow-derived hMSCs were kindly provided by Tulane University Health Sciences Center. The culture medium used was  $\alpha$ -minimum essential medium with fetal bovine serum (20%) and penicillin/streptomycin (1%) at 37 °C and 5% CO<sub>2</sub>. The 3–5 th passages of the hMSCs were used in this study. To encapsulate hMSC in DE droplets, hMSC were trypsinized and suspended at (2, 5, 10, 20\* 10<sup>5</sup> cell/mL) in culture medium supplemented with Pluronic® F-127 (1 wt%) (Sigma-Aldrich, St. Louis, MO). The flow rates of three phases (inner aqueous: middle oil: outer aqueous) were set at 5 : 10 : 25 µL/min respectively. The droplets were collected and transferred to 24-well plates for subsequent culture and analysis.

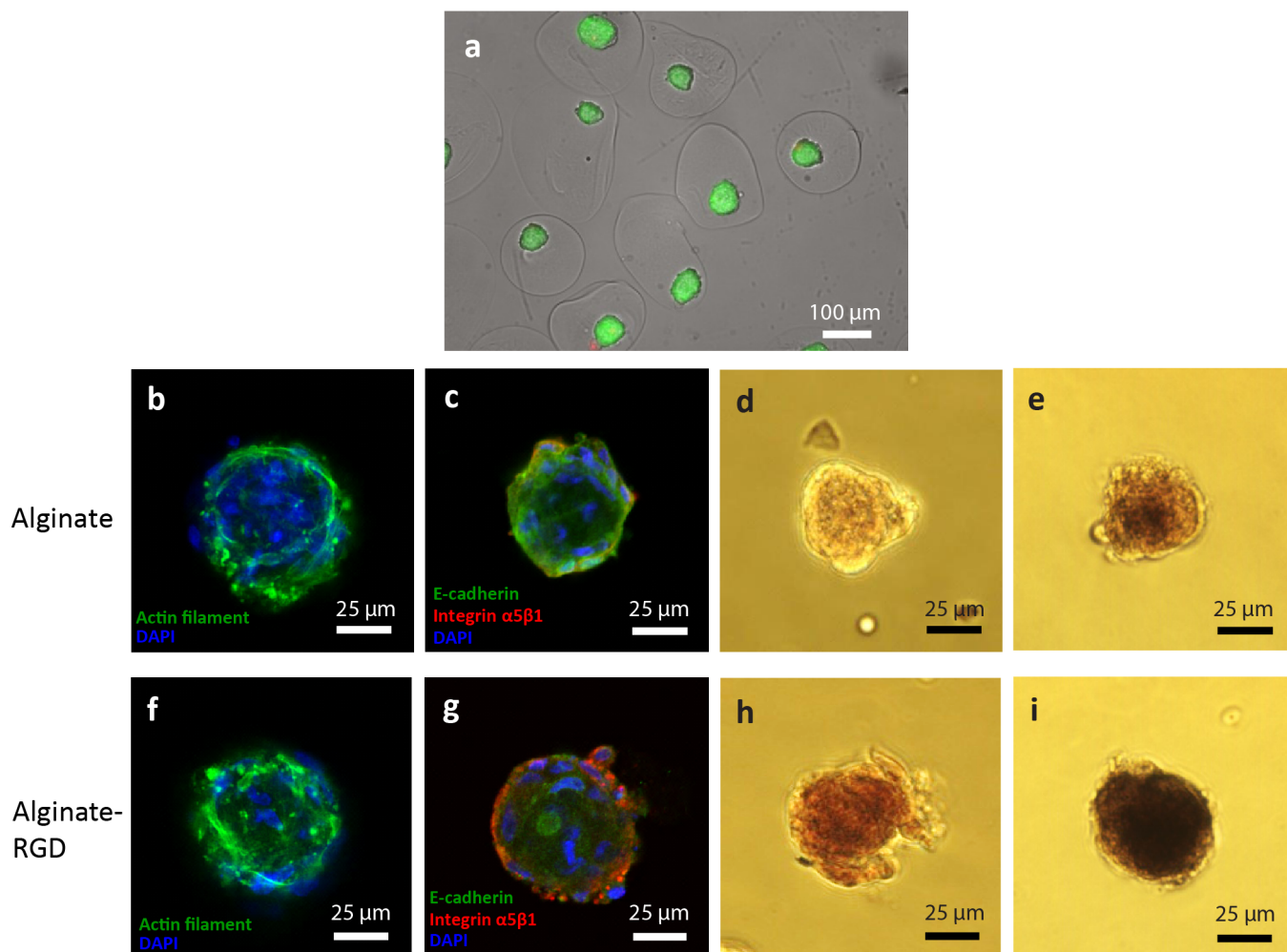


**Figure 4 | Control of microenvironment for spheroid culture using DE droplets.** (a) Live/dead staining of spheroids encapsulated in alginate gel. Live and dead cells were stained with calcein AM (green) and propidium iodide (red) respectively. Confocal images showing phalloidin staining (b, f) and immunostaining for E-cadherin, integrin  $\alpha 5 \beta 1$  (c, g) for spheroids encapsulated in alginate or alginate-RGD gel cultured in normal media for 3 days. Images of alizarin red staining (d, h) and alkaline phosphatase activity staining using BCIP/NBT as substrate (e, i) for spheroids cultured in osteogenic medium for 7 days.

**hMSC spheroid characterization.** The frequency of spheroid formation was determined by counting the number of DE droplets containing a spheroid from the pool of 50–150 droplets each time. The hMSC spheroids were released from the DE droplets using a droplet releasing agent (1H,1H,2H,2H-Perfluoro-1-octanol from Sigma-Aldrich, St. Louis, MO). In a sterilized microcentrifuge tube, the droplet releasing agent (50  $\mu\text{L}$ ), PBS (200  $\mu\text{L}$ ) and DE droplets (variable volume) were added sequentially and left at room temperature for two minutes. The aqueous phase was then retrieved which contained released hMSC spheroids. The retrieval yield was determined by counting the number of intact droplets remained after the droplet release process using an initial droplet number of 100–300. The viability of hMSC spheroids was determined qualitatively by staining the spheroids with calcein AM and propidium iodide. The area of live cell (green) was divided by the total area of spheroids (green + red) to determine the ratios of live cell area in the spheroids. The hMSC spheroids were cultured on either TCPS or ultra-low attachment multiwell plate (Corning, Tewksbury, MA) to determine cell migration from the spheroids. The released spheroids and hMSC culture on TCPS were cultured in adipogenic differentiation medium (Lonza, Walkersville, MD) for 7 days before fixed with paraformaldehyde (4%) and stained with Oil Red O solution (Sigma-Aldrich, St. Louis, MO). For immunostaining, paraformaldehyde-fixed hMSC spheroids were stained with collagen type I (Abcam, Cambridge, MA) and laminin (Abcam, Cambridge, MA) antibodies. Different Alexa Fluor secondary antibodies (Abcam, Cambridge, MA) were used to obtain fluorescent colors. The stained samples were analyzed under an inverted confocal microscope (Zeiss LSM 510) available at Duke Light Microscopy Core Facility.

**Formation of PMEF, Caco-2 and HepG2 spheroids.** PMEF (passage number = 4), Caco-2 (passage number = 45) and HepG2 cells (passage number = 90) were obtained from ATCC (Manassas, VA) and Duke Cell Culture Facility and cultured according to supplier's recommendation. Each cell type was trypsinized and

resuspended at  $8 \times 10^6$  cells/mL and encapsulated in DE droplets. Bright-field images were taken at 2 hr and 6 hr (in the case of Caco-2) after droplet formation.

**Encapsulation of hMSC spheroids in hydrogel.** It followed the same procedures as generating hMSC spheroids except the trypsinized cells were suspended in alginate (1%) (PRONOVA SLG100, Novamatrix) or alginate-RGD (1%) (NOVATACH-G-RGD, Novamatrix) solution. After spheroids were formed, the gelation of inner phase was carried out by adding the droplet releasing agent (50  $\mu\text{L}$ ),  $\text{CaCl}_2$  (200 mM) in NaCl solution (200  $\mu\text{L}$ , 150 mM) and DE droplets (variable volume) sequentially in a sterilized microcentrifuge tube and left at room temperature for two minutes. The retrieved microgels were washed with NaCl solution (150 mM) twice before transferred to cell culture medium for subsequent culture.

**Osteogenic differentiation and characterization.** Osteogenic differentiation of hMSC spheroids encapsulated in hydrogel was performed using optimized differentiation medium (StemPro<sup>®</sup> Osteogenesis Differentiation Kit, Life Technologies, Grand Island, NY) following manufacturer's protocol. To perform Alizarin red staining, samples were fixed in 4% paraformaldehyde before washed with water. Alizarin red solution (0.02%) (Sigma-Aldrich, St. Louis, MO) with pH adjusted to 4.1–4.3 was prepared in distilled water. Samples were stained in the solution for 45 min before washed with PBS and analyzed under light microscope. Staining of alkaline phosphatase activity by using BCIP/NBT as substrate (SigmaFast<sup>™</sup> BCIP-NBT; Sigma Aldrich, St. Louis, MO) was carried out following manufacturer's protocol before the samples were analyzed under light microscope.

1. Baraniak, P. R. & McDevitt, T. C. Scaffold-free culture of mesenchymal stem cell spheroids in suspension preserves multilineage potential. *Cell Tissue Res* **347**, 701–711 (2012).



2. Bosenberg, M. W. & Massague, J. Juxtacrine cell signaling molecules. *Curr Opin Cell Biol* **5**, 832–838 (1993).
3. Korff, T. & Augustin, H. G. Integration of endothelial cells in multicellular spheroids prevents apoptosis and induces differentiation. *J Cell Biol* **143**, 1341–1352 (1998).
4. Lu, H. F. *et al.* Three-dimensional co-culture of rat hepatocyte spheroids and NIH/3T3 fibroblasts enhances hepatocyte functional maintenance. *Acta Biomater* **1**, 399–410 (2005).
5. Bosnakovski, D. *et al.* Chondrogenic differentiation of bovine bone marrow mesenchymal stem cells (MSCs) in different hydrogels: influence of collagen type II extracellular matrix on MSC chondrogenesis. *Biotechnol Bioeng* **93**, 1152–1163 (2006).
6. Langenbach, F. *et al.* Scaffold-free microtissues: differences from monolayer cultures and their potential in bone tissue engineering. *Clin Oral Investig* **17**, 9–17 (2013).
7. Huang, Y. C. *et al.* Scalable production of controllable dermal papilla spheroids on PVA surfaces and the effects of spheroid size on hair follicle regeneration. *Biomaterials* **34**, 442–451 (2013).
8. Kelm, J. M. *et al.* Tissue-transplant fusion and vascularization of myocardial microtissues and macro-tissues implanted into chicken embryos and rats. *Tissue Eng* **12**, 2541–2553 (2006).
9. Schon, B. S. *et al.* Validation of a high-throughput microtissue fabrication process for 3D assembly of tissue engineered cartilage constructs. *Cell Tissue Res* **347**, 629–642 (2012).
10. Kelm, J. M. *et al.* Design of custom-shaped vascularized tissues using microtissue spheroids as minimal building units. *Tissue Eng* **12**, 2151–2160 (2006).
11. Wang, W. *et al.* 3D spheroid culture system on micropatterned substrates for improved differentiation efficiency of multipotent mesenchymal stem cells. *Biomaterials* **30**, 2705–2715 (2009).
12. Schukur, L., Zorlutuna, P., Cha, J. M., Bae, H. & Khademhosseini, A. Directed differentiation of size-controlled embryoid bodies towards endothelial and cardiac lineages in RGD-modified poly(ethylene glycol) hydrogels. *Adv Healthc Mater* **2**, 195–205 (2013).
13. Lim, S. H. & Mao, H. Q. Electrospun scaffolds for stem cell engineering. *Adv Drug Deliv Rev* **61**, 1084–1096 (2009).
14. Kitagawa, F., Takei, S., Imaizumi, T. & Tabata, Y. Chondrogenic Differentiation of Immortalized Human Mesenchymal Stem Cells on Zirconia Microwell Substrata. *Tissue Eng Part C Methods* **19**, 438–448 (2012).
15. Dawson, E., Mapii, G., Erickson, K., Taqvi, S. & Roy, K. Biomaterials for stem cell differentiation. *Adv Drug Deliv Rev* **60**, 215–228 (2008).
16. Bian, L., Guvendiren, M., Mauck, R. L. & Burdick, J. A. Hydrogels that mimic developmentally relevant matrix and N-cadherin interactions enhance MSC chondrogenesis. *Proc Natl Acad Sci U S A* **110**, 10117–10122 (2013).
17. Shin, S. R. *et al.* Cell-laden Microengineered and Mechanically Tunable Hybrid Hydrogels of Gelatin and Graphene Oxide. *Adv Mater* (2013).
18. Chung, C. & Burdick, J. A. Influence of three-dimensional hyaluronic acid microenvironments on mesenchymal stem cell chondrogenesis. *Tissue Eng Part A* **15**, 243–254 (2009).
19. Yang, F. *et al.* The effect of incorporating RGD adhesive peptide in polyethylene glycol diacrylate hydrogel on osteogenesis of bone marrow stromal cells. *Biomaterials* **26**, 5991–5998 (2005).
20. Lin, R. Z. & Chang, H. Y. Recent advances in three-dimensional multicellular spheroid culture for biomedical research. *Biotechnol J* **3**, 1172–1184 (2008).
21. Lee, E. J. *et al.* Spherical bullet formation via E-cadherin promotes therapeutic potency of mesenchymal stem cells derived from human umbilical cord blood for myocardial infarction. *Mol Ther* **20**, 1424–1433 (2012).
22. Kurosawa, H. Methods for inducing embryoid body formation: in vitro differentiation system of embryonic stem cells. *J Biosci Bioeng* **103**, 389–398 (2007).
23. Tung, Y. C. *et al.* High-throughput 3D spheroid culture and drug testing using a 384 hanging drop array. *Analyst* **136**, 473–478 (2011).
24. Faulkner-Jones, A. *et al.* Development of a valve-based cell printer for the formation of human embryonic stem cell spheroid aggregates. *Biofabrication* **5**, 015013 (2013).
25. Choi, Y. Y. *et al.* Controlled-size embryoid body formation in concave microwell arrays. *Biomaterials* **31**, 4296–4303 (2010).
26. Lee, K. H. *et al.* Diffusion-mediated in situ alginate encapsulation of cell spheroids using microscale concave well and nanoporous membrane. *Lab Chip* **11**, 1168–1173 (2011).
27. Ungrin, M. D., Joshi, C., Nica, A., Bauwens, C. & Zandstra, P. W. Reproducible, ultra high-throughput formation of multicellular organization from single cell suspension-derived human embryonic stem cell aggregates. *PLoS One* **3**, e1565 (2008).
28. Hung, P. J., Lee, P. J., Sabounchi, P., Lin, R. & Lee, L. P. Continuous perfusion microfluidic cell culture array for high-throughput cell-based assays. *Biotechnol Bioeng* **89**, 1–8 (2005).
29. Myers, F. B., Henrikson, R. H., Xu, L. & Lee, L. P. A point-of-care instrument for rapid multiplexed pathogen genotyping. *Conf Proc IEEE Eng Med Biol Soc* **2011**, 3668–3671 (2011).
30. Wu, H. W., Lin, C. C. & Lee, G. B. Stem cells in microfluidics. *Biomicrofluidics* **5**, 13401 (2011).
31. Chang, C. M., Chiu, L. F., Wang, P. W., Shieh, D. B. & Lee, G. B. A microfluidic system for fast detection of mitochondrial DNA deletion. *Lab Chip* **11**, 2693–2700 (2011).
32. Juul, S. *et al.* Detection of single enzymatic events in rare or single cells using microfluidics. *ACS Nano* **5**, 8305–8310 (2011).
33. Yang, S. *et al.* Microfluidic synthesis of multifunctional Janus particles for biomedical applications. *Lab Chip* **12**, 2097–2102 (2012).
34. Griffiths, A. D. & Tawfik, D. S. Miniaturising the laboratory in emulsion droplets. *Trends Biotechnol* **24**, 395–402 (2006).
35. Li, S. *et al.* An on-chip, multichannel droplet sorter using standing surface acoustic waves. *Anal Chem* **85**, 5468–5474 (2013).
36. Chen, F. *et al.* Chemical transfection of cells in picoliter aqueous droplets in fluorocarbon oil. *Anal Chem* **83**, 8816–8820 (2011).
37. Zhang, Y. *et al.* A programmable microenvironment for cellular studies via microfluidics-generated double emulsions. *Biomaterials* **34**, 4564–4572 (2013).
38. Yoon, S., Kim, J. A., Lee, S. H., Kim, M. & Park, T. H. Droplet-based microfluidic system to form and separate multicellular spheroids using magnetic nanoparticles. *Lab Chip* **13**, 1522–1528 (2013).
39. Yu, L., Chen, M. C. & Cheung, K. C. Droplet-based microfluidic system for multicellular tumor spheroid formation and anticancer drug testing. *Lab Chip* **10**, 2424–2432 (2010).
40. Sakai, S. *et al.* Cell-enclosing gelatin-based microcapsule production for tissue engineering using a microfluidic flow-focusing system. *Biomicrofluidics* **5**, 13402 (2011).
41. Yu, J. *et al.* The use of human mesenchymal stem cells encapsulated in RGD modified alginate microspheres in the repair of myocardial infarction in the rat. *Biomaterials* **31**, 7012–7020 (2010).
42. Jeong, G. S. *et al.* Surface tension-mediated, concave-microwell arrays for large-scale, simultaneous production of homogeneously sized embryoid bodies. *Adv Healthc Mater* **2**, 119–125 (2013).
43. Lee, W. Y. *et al.* The use of injectable spherically symmetric cell aggregates self-assembled in a thermo-responsive hydrogel for enhanced cell transplantation. *Biomaterials* **30**, 5505–5513 (2009).
44. Luebke-Wheeler, J. L., Nedredal, G., Yee, L., Amiot, B. P. & Nyberg, S. L. E-cadherin protects primary hepatocyte spheroids from cell death by a caspase-independent mechanism. *Cell Transplant* **18**, 1281–1287 (2009).
45. Takagi, J., Strokovich, K., Springer, T. A. & Walz, T. Structure of integrin alpha5beta1 in complex with fibronectin. *EMBO J* **22**, 4607–4615 (2003).
46. Donzelli, E. *et al.* Mesenchymal stem cells cultured on a collagen scaffold: In vitro osteogenic differentiation. *Arch Oral Biol* **52**, 64–73 (2007).
47. Kim, C. *et al.* Generation of core-shell microcapsules with three-dimensional focusing device for efficient formation of cell spheroid. *Lab Chip* **11**, 246–252 (2011).
48. Maguire, T., Novik, E., Schloss, R. & Yarmush, M. Alginate-PLL microencapsulation: effect on the differentiation of embryonic stem cells into hepatocytes. *Biotechnol Bioeng* **93**, 581–591 (2006).
49. Hernandez, R. M., Orive, G., Murua, A. & Pedraz, J. L. Microcapsules and microcarriers for in situ cell delivery. *Adv Drug Deliv Rev* **62**, 711–730 (2010).
50. Reiss, J. G. & Krafft, M. P. Advanced fluorocarbon-based systems for oxygen and drug delivery, and diagnosis. *Artif Cells Blood Substit Immobil Biotechnol* **1**, 43–52 (1997).
51. Holt, D. J., Payne, R. J. & Abell, C. Synthesis of novel fluorosurfactants for microdroplet stabilisation in fluorosurfactant streams. *Journal of Fluorine Chemistry* **131**, 398–407 (2010).
52. Clausell-Tormos, J. *et al.* Droplet-based microfluidic platforms for the encapsulation and screening of Mammalian cells and multicellular organisms. *Chem Biol* **15**, 427–437 (2008).
53. Matsunaga, Y. T., Morimoto, Y. & Takeuchi, S. Molding cell beads for rapid construction of macroscopic 3D tissue architecture. *Adv Mater* **23**, H90–94 (2011).
54. Mironov, V. *et al.* Organ printing: tissue spheroids as building blocks. *Biomaterials* **30**, 2164–2174 (2009).
55. Lin, R. Z., Chu, W. C., Chiang, C. C., Lai, C. H. & Chang, H. Y. Magnetic reconstruction of three-dimensional tissues from multicellular spheroids. *Tissue Eng Part C Methods* **14**, 197–205 (2008).
56. Burdick, J. A. & Vunjak-Novakovic, G. Engineered microenvironments for controlled stem cell differentiation. *Tissue Eng Part A* **15**, 205–219 (2009).
57. Hong, S., Hsu, H. J., Kaunas, R. & Kameoka, J. Collagen microsphere production on a chip. *Lab Chip* **12**, 3277–3280 (2012).
58. Tumarkin, E. & Kumacheva, E. Microfluidic generation of microgels from synthetic and natural polymers. *Chem Soc Rev* **38**, 2161–2168 (2009).
59. Eun, Y. J., Utada, A. S., Copeland, M. F., Takeuchi, S. & Weibel, D. B. Encapsulating bacteria in agarose microparticles using microfluidics for high-throughput cell analysis and isolation. *ACS Chem Biol* **6**, 260–266 (2011).
60. Chia, S. M. *et al.* Engineering microenvironment for expansion of sensitive anchorage-dependent mammalian cells. *J Biotechnol* **118**, 434–447 (2005).

## Acknowledgments

The work was supported by UH2TR000505 and the NIH Common Fund for the Microphysiological Systems Initiative, and by EB015300. H.F.C. and Y.Z. are grateful for



fellowship support from the Sir Edward Youde Memorial Fund Council (Hong Kong) and the Agency for Science, Technology and Research (Singapore), respectively. Y.P.H. would like to acknowledge funding support from Danish Research Councils (11-116325/FTP) and Karen Elise Jensen Foundation. The authors thank Siying Ma for composing Figure 1c.

### Author contributions

H.F.C., Y.P.H. and K.W.L. conceived and designed the experiments; H.F.C., Y.Z., Y.L.C. and Y.J. performed the experiments; H.F.C. and K.W.L. analyzed the data; H.F.C. and K.W.L. wrote the manuscript.

### Additional information

**Supplementary information** accompanies this paper at <http://www.nature.com/scientificreports>

**Competing financial interests:** The authors declare no competing financial interests.

**How to cite this article:** Chan, H.F. *et al.* Rapid formation of multicellular spheroids in double-emulsion droplets with controllable microenvironment. *Sci. Rep.* **3**, 3462; DOI:10.1038/srep03462 (2013).



This work is licensed under a Creative Commons Attribution-NonCommercial-NoDerivs 3.0 Unported license. To view a copy of this license, visit <http://creativecommons.org/licenses/by-nc-nd/3.0>